Advances in Nanochemistry

Article

Potential-modulated release of ceftriaxone using chitosan hydrogel-based composite involving ordered mesoporous carbon and graphene

Received 11th December 2019,
Accepted 8th January 2020,
DOI:10.22126/anc.2020.4839.1019

Toraj Ahmadi-Jouibari [1], Mari Ataee [1], Negar Noori [1], Nazir Fattahi *[,2]

[1] Clinical Research Development Center, Imam Khomeini and Dr. Mohammad Kermanshahi and Farabi Hospitals, Kermanshah University of Medical Sciences, Kermanshah, Iran.

[2] Research Center for Environmental Determinants of Health (RCEDH), Health Institute, Kermanshah University of Medical Sciences, Kermanshah, Iran.

Abstract

We report on the successful release-modulation of ceftriaxone (CEF) by an applied potential on a chitosan hydrogel-based composite. Here, the performance of chitosan (CHIT)-based composites were evaluated on glassy carbon electrode (GC), GC-ordered mesoporous carbons (OMCs) and Graphene (Gr), which offer attractive features such as good electronic conductivity and effectiveness in delivering electroactive surface area. Ceftriaxone was selected as an indicator of cephalosporins as a model drug. Besides this, based on the fact that CEF has three p*Ka*, we carefully studied the electronic structures, hardness, and HOMO-LUMO gaps of deprotonated forms, for the first time, using DFT-B3LYP/6-31G* method. The optimized structures of the anions 1, 2, and 3 implied that the proton (H^+), located in an electronic sponge, changes its position from -COO^-, in anion 1 to -NH_3^+ in anions 2 and 3. Due to its porous morphology and high surface area, the prepared OMCs/CHIT film found to have a significantly higher capability in the time-controlled release of the CEF and prevention of its fast depletion into the aqueous medium, compared to GR/CHIT and GC/CHIT films.

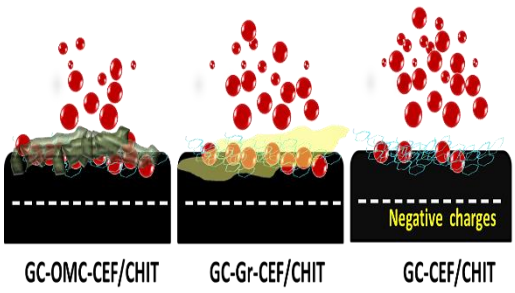

Keywords: *Ordered mesoporous carbons, Graphene, Chitosan, Electrochemically-controlled drug release, Cephalosporins.*

Introduction

Noninvasive externally controlled drug release systems are of increasing interest since they allow repeatable and reliable remote off-on switching of drug release. These systems are comprised of a drug, an external stimulus, stimulus-sensitive materials, and stimulus-responsive carriers. The external stimulus can be light,[1,2] magnetic field,[3,4] ultrasound, and radiofrequency.[5] However, the problem with current conventional methods for introducing medicines into the body is that a maximum dose of the drug is initially supplied, while the dosage is dramatically decreased over a short period of time.

In fact, an ideal design of a drug delivery system is expected to respond to the physiological conditions such as body temperature, changes in pH conditions, hormonal concentration levels, blood glucose level, electrical pulses, and so on.[6-9] Thus, the electrical stimulation to affect the localized and controlled release of therapeutic drugs has become an attractive option in the treatment of acute diseases or chronic illnesses. Here, such electrical parameters as pulse type, amplitude, polarity, and duration can be easily adapted to control the drug release step. The application of carbon-material based systems was attended in diverse electrically stimulated drug release systems.[6,10,11]

Naficy and co-workers described the modulated release of dexamethasone (DEX) by electrical stimulation that was investigated using chitosan (CHIT) and single-walled carbon nanotubes (SWCNT) host carrier films.[6] Recently, Weaver et. al, extended an electrically controlled drug delivery system based on a conductive nanocomposite film composed of poly(pyrrole) (PPy) doped with GO a nanosheets for controlled delivery of anti-inflammatory drugs.[11] In another work, hybrid hydrogel membranes composed of reduced graphene oxide (rGO) nanosheets and a poly(vinyl alcohol) (PVA) matrix were established as an electrically responsive drug release system for anesthetic drug, lidocaine hydrochloride.[10]

Carbon nanomaterials with unique nanostructure are the most studied materials in nanotechnology, despite some conflicting results about their safety profiles. Although their structures are simple, carbon nanomaterials provide exceptional physical and chemical properties including high electrical and thermal conductivities, unique optical properties, and extreme chemical stability. Accordingly, both graphene and ordered mesoporous carbons (OMCs) shown the unique properties in research works. Graphene, as a new class of two-dimensional nanomaterial consisting of a single layer of sp^2 network of carbon atoms, has inspired wide interests in both the experimental and theoretical scientific community due to its extraordinary electrical, mechanical, and thermal properties.[12] OMCs are biquitous and indispensable in many modern-day scientific applications. Their use in diverse applications is directly related not only to their superior physical

Corresponding author:
Nazir Fattahi, Email: nazirfatahi@yahoo.com

and chemical properties, such as electric conductivity, thermal conductivity, chemical stability, and low density but also to their wide availability. These unique features offer graphene and OMCs great promise for many practical applications including drug delivery.[13-15]

Because of its biocompatibility, chitosan has been of widespread interest in designing drug delivery systems. Chitosan hydrogels have been used as a matrix to control the delivery of different drug molecules by electrical stimulation.[16] However, in the case of such insulating materials, the applied potential for the drug release can reach up to several tens of volts, while the applied current can be a few milliamperes.[17] Since high voltage conditions cannot be tolerated *in vivo*, the developed strategies require enhancement of the material conductivity to stimulate the drug release at lower overpotentials. In this respect, the incorporation of conductive nano-sized carbon materials in drug delivery systems is quite desirable.[18,19] Moreover, a part of this work concentrated on exploring structural and electrical features of ceftriaxone anions in different subsequent anions forms that give us a good insight for other similar structures for establishing next innovative research works. In this work, we compared the chitosan (CHIT) composites modified with ordered mesoporous carbons (OMCs), graphene (GR), and glassy carbon (GC) as matrices for electrically modulated release of ceftriaxone (CEF), as a model drug.

Experimental

Chemicals and apparatus

Ceftriaxone sodium (See Figure 1) was purchased from Sandoz Pharmaceutical Co. Ltd. (Frankfurt, Germany). SBA-15 was obtained from Sigma-Aldrich. All other chemicals were of analytical grade from Merck and used as received. All cyclic voltammetric (CV) and electrochemical impedance spectroscopic (EIS) measurements were carried out with a computer-controlled μ-Autolab type III potentiostat (Eco Chemie, Utrecht, the Netherlands) and run with the GPES software in conjunction with a conventional three-electrode system and a personal computer for data storage and processing. The UV-Vis spectra of releasing CEF were recorded by an Agilent 8453 spectrophotometer (California, USA).

Synthesis of OMC and Graphene

OMCs were prepared according to the method reported by Ryoo and coworkers.[20] The synthesis was performed using SBA-15 silica as the template and sucrose as the carbon source. In brief, 1 g of SBA-15 was added to the solution of sucrose (1.25 g) and 0.14 g of H_2SO_4 in 5 mL of H_2O, the mixture was placed in oven for 5 h at 100 °C, and subsequently, the oven temperature was increased to 165 °C and maintained there for 5 h. The sample turned black during this step. Next, the silica sample, containing partially polymerized and carbonized sucrose, after the addition of 0.8 g of sucrose, 0.09 g of H_2SO_4, and 5 mL of H_2O, was treated again at 100 °C and 160 °C. The carbonization was completed by pyrolysis with heating to typically 900 °C under vacuum. The carbon-silica composite obtained after pyrolysis was washed with 1 M NaOH solution (water:ethanol, 50%:50%) twice at 95 °C and 5 wt.% hydrofluoric acid at room temperature (RT), to remove the silica template. The template-free carbon product thus obtained was filtered, washed with ethanol, and dried at 110 °C.

Graphene was synthesized from graphite by the modified Hummers' method.[21,22] For the improved method, a mixture 9:1 of concentrated H_2SO_4/H_3PO_4 (360:40 mL) was added to a mixture of 3.0 g of graphite flakes, and $KMnO_4$ (18.0 g), producing a slight exotherm to *ca.* 40 °C. The reaction was then heated to 55 °C and stirred for 11 h. The reaction was cooled to RT and poured onto ice (400 mL) with 30% H_2O_2 (3 mL). Next, the mixture was then filtered, centrifuged at 3500 rpm and the supernatant was decanted away. The residual solid was washed in succession with 300 mL of water, 300 mL of 30% HCl, and 300 mL of ethanol. The solid obtained on the filter was vacuum-dried overnight at room temperature.

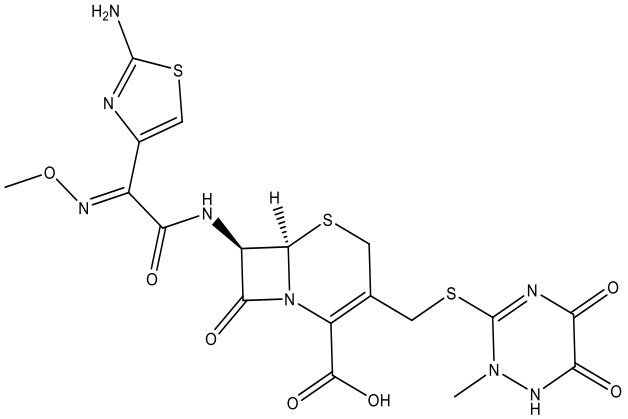

Figure 1. *The molecular structure of ceftriaxone.*

Loading of composites

Ceftriaxone sodium powder was added to an aqueous solution containing 1.0 wt.% of carbon material (i.e., OMCs and GR) and 0.4 wt.% of CHIT in water and sonicated for 40 min. Then, drop cast films were obtained by carefully pipetting 10 μL of the solution onto a GCE and allowed to dry overnight. The concentration of released CEF was measured from a standard spectrophotometric curve of known CEF concentrations.

Electrochemically-controlled drug release

The electrochemically-controlled release of CEF from the composite films was carried out in a small electrochemical cell containing 5.0 mL of 0.05 M phosphate buffer solution (PBS) of pH 6.2. The drug release was studied at different composite electrodes over a potential window of 0.1 to -1.1 V. A portion of solution with released drug was then transferred to UV-Vis cell for CEF assay at 260±3 nm and after each specific time interval, using a calibration curve. The cumulative amount of CEF released was obtained from the amount of drug in the release media before and after a given time interval. The percentage of CEF release was calculated based on the initial amount of CEF in the film.

Results and discussion

The SEM images shown in Figure 2A and 2B confirm the previously reported structures for GR[25] and OMCs,[22] respectively. CV and EIS were used to compare the electroactivity between CEF-CHIT/GCE, CEF-GR/CHIT/GCE, CEF-OMCs/CHIT/GCE, and CEF-OMCs/GCE using $[Fe(CN)_6]^{3-/4-}$ system as a redox probe and the results are shown in Figure 3A and B, respectively. The modification of GCE by different CEF-carbon material-CHIT composites leads to changes in current density, charge-transfer resistance (R_{ct}), and peak-to-peak separation (ΔE_p). As is obvious from Figure 3A, a pair of well-defined $[Fe(CN)_6]^{3-/4-}$ redox peak was observed at these electrodes, but with different peak currents and peak-to-peak separations.

The ΔE_p values at (a) CEF/CHIT/GCE, (b) GR-CEF/CHIT/GCE, (c) OMCs-CEF/GCE, and (d) OMCs-CEF/CHIT/GCE are 632, 344, 105, and 346 mV, respectively (Figure 3). As it is seen, a pair of redox peaks with much lower ΔE_p was observed for OMCs-CEF/GCE (curve c). Curve d, however, points out the striking influence of the positively charged chitosan in OMCs-CEF/CHIT/GCE. It shows that, because of electrostatic attraction between positively-charged

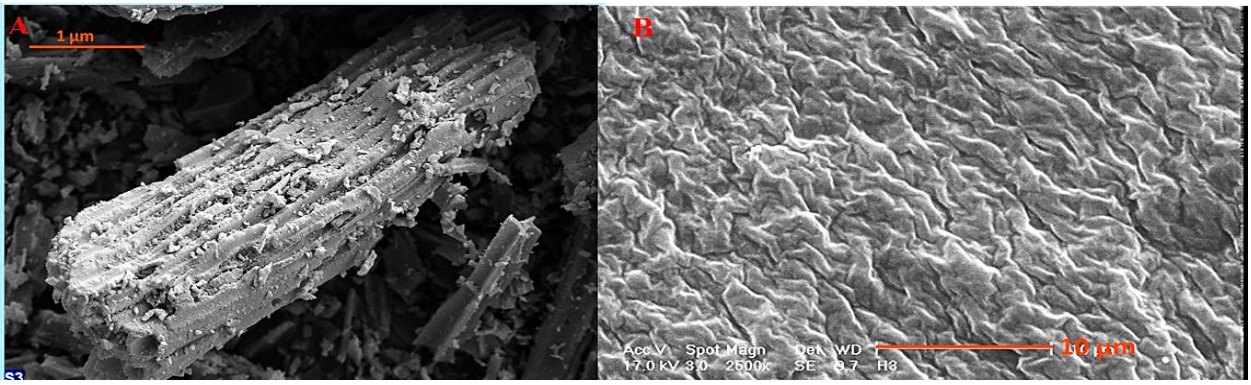

Figure 2. *The SEM images of (A) OMCs and (B) GR.*

chitosan and negatively-charged $[Fe(CN)_6]^{3-/4-}$ redox probe, a larger peak current obtained at OMCs-CEF/CHIT/GCE. On the other hand, the ΔE_p in OMCs-CEF/CHIT/GCE largely increased compared to that in OMCs-CEF/GCE, which is due to the insulating properties of CHIT present at the surface of the electrode. Close ΔE_p values of GR-CEF/CHIT/GCE and OMCs-CEF/CHIT/GCE confirmed their more or less similar charge transfer properties. However, the peak current intensity on the OMCs modified electrodes (c and d) was much larger than that of the two other GR and GC modified electrodes, under the same operating conditions, due to porous morphology and high surface area of OMCs, compared to GR and GC. As it is clear from Figure 3B, the R_{ct} values obtained from EIS measurements were in accordance with the CV results of the $[Fe(CN)_6]^{3-/4-}$ redox probe in the solution.

In the next step, the electroactive surface areas of the bare GCE and that modified with chitosan composites of OMCs, GR and GC were obtained according to the Randles–Sevcik equation:[23,24]

$$i_p = (2.69 \times 10^5)\, AD^{1/2} n^{3/2} \upsilon^{1/2} C^* \quad (1)$$

According to this equation, the average value of the electroactive surface area for OMCs-CEF/CHIT/GCE, GR-CEF/CHIT/GCE, and CEF/CHIT/GCE found to be 0.103, 0.066, and 0.044 cm^2, respectively, clearly emphasizing that the OMCs-CEF/CHIT/GCE possesses a much larger effective surface area, which is expected to result in rather high capacitive currents. As obviously observed from Figure 4, the OMCs-CEF/CHIT/GCE has a larger capacitive current (curve c) compared to the GR-CEF/CHIT/GCE (curve b) and CEF/CHIT/GCE (curve a) electrodes.

The drug release of different systems was also examined, in order to investigate the capability of their controlled drug loading/release, and the results are shown in Figure 5. By comparing the amount of drug release with time from the OMCs-CEF/CHIT/GCE electrode with that from the GR-CEF/CHIT/GCE and CEF/CHIT/GCE electrodes, it can be seen that the existence of GR and, especially, OMCs in the designed electrode systems will result in significantly high capability of the corresponding chitosan composites in time-controlled release of the drug and prevention of its fast depletion into the aqueous medium. In fact, in contrast to conventional drug delivery systems, the incorporation of conductive nano-sized carbon materials in drug delivery processes not only facilitates an extra drug loading, but also increases the control over electrical release of the drug with time. In the absence of such carbon nanomaterials, the drug dropped on the electrode surface can be easily washed out during the immersing in aqueous media and scanning of potential.

The effect of amount of applied electrical potential on the release of drug was also investigated and the results are shown in Figure 6. The results show that, as expected, an increase in the applied potential causes a significant increase in release of CEF with time. Since the resultant charge of CEF is negative in pH values 6 to 7, it can be postulated that a negative potential applied to the electrode further enhances the rate of CEF release via an electro-repulsion process. Applying a negative potential of -1.1 V to the carbon substrate of the CHIT composites produced a higher CEF release of about 100% (vs. 55% for the un-stimulated sample),

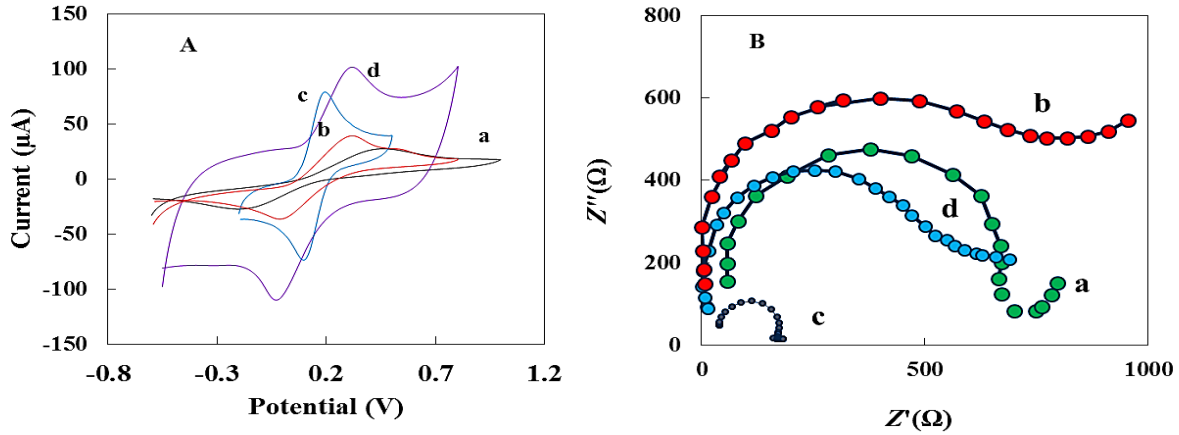

Figure 3. *The respective (A) CVs and (B) EIS of (a) GCE, (b) CEF-GR/CHIT/GCE, (c) CEF-OMCs/GCE and, (d) CEF-OMCs/CHIT/GCE in the presence of 5.0 mM $[Fe(CN)_6]^{3-/4-}$ and 0.1 M KCl at pH 6.0.*

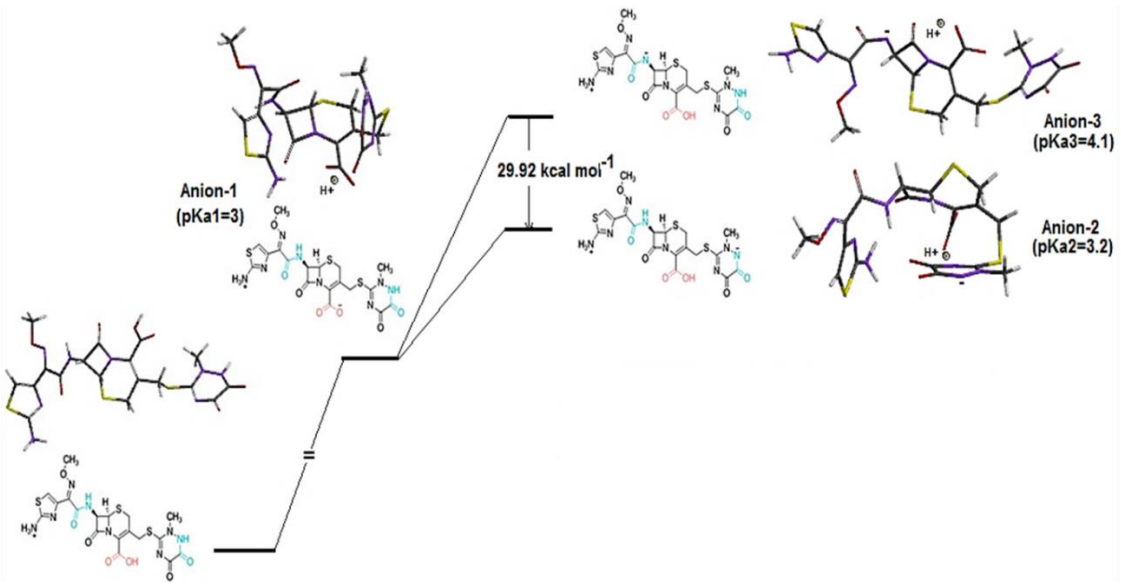

Scheme 1. *The Proposed mechanism of successive proton dissociation reactions of CEF.*

when monitored over 24 h. Figure 7 shows the typical UV-Vis spectra of stimulated drug release at -1.1 V with elapse of time from the OMC-CEF/CHIT/GCE.

Figure 8 shows the effect of solution pH on the release of CEF from OMC-CEF/CHIT/GCE. For a drug like CEF with both acidic and basic functional groups, the cationic and anionic forms are expected to be dominant in different ranges of pH. CEF has a highly polar structure and possesses three acidic protons attributed to one carboxylic and two carbonamido groups and may exist with different charges depending on the pH range of the solution (see Scheme 1).

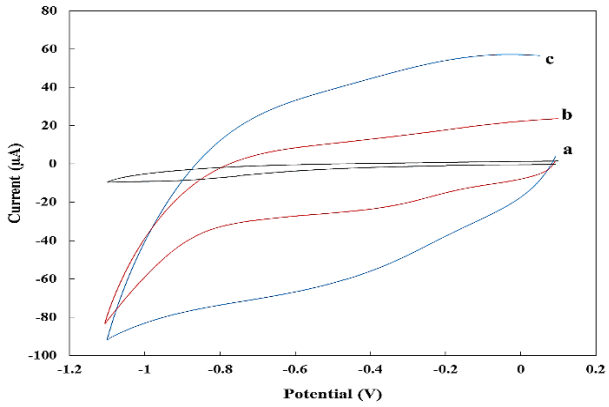

Figure 4. *CVs of (a) CEF-CHIT/GCE, (b) CEF-GR/CHIT/GCE, and (c) CEF-OMCs/CHIT/GCE in phosphate buffer of pH 6.2 at a scan rate of 50 mV s^{-1}.*

The pK_a values of CEF are 3.0, 3.2, and 4.1.[25] The pK_{a1} is related to the carboxylic group proton, whereas the remaining pK_a values (pK_{a2} and pK_{a3}) are assigned to the carbonamido groups present in its structure. The CEF structures with different pK_a were optimized by density functional theory/Becke-3–Lee–Yang–Parr (DFT-B3LYP) method and 6-31G* basis set using the Spartan '10 package and the results together with the corresponding calculated energy levels are also added to Scheme 1. The results revealed that the CEF anion 1 with a pK_a of 3.0 is the most stable anion. In comparison, this anion is more stable than the two other anions (i.e., 2 and 3). The DFT-B3LYP/6-31G* calculations showed that the anion 2 is 29.9 kcal mol^{-1} more stable than the anion 3. So, pK_a= 3.2 and 4.1 are related to anions 2 and 3, respectively. The HOMO and LUMO gap of the anions 1, 2, and 3 are 3.72, 3.54, and 2.31 eV, respectively, and the respective hardness of the anions are 1.86, 1.77, and 1.15 eV. Thus, it seems that the pK_a decreases with increasing the HOMO-LUMO gap and the hardness of the anions.

The optimized structures of the anions 1, 2, and 3 show that the proton (H^+), located in an electronic sponge, changes its position from $-COO^-$, in anion 1 to $-NH_3^+$ in anions 2 and 3. The different folded structures observed in the optimized cases of the CEF anions 1-3 are related to such parameters as wrapping around the possibility of the delocalized proton, the internal hydrogen bonding, and steric and electrostatic effects at the CEF anion structures.

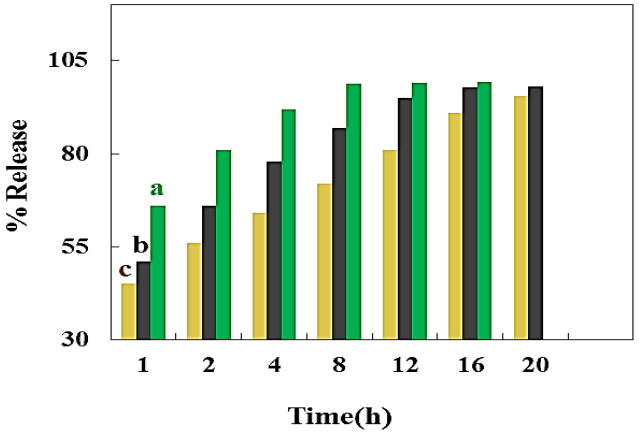

Figure 5. *Cumulative drug release from (a) CEF/CHIT/GCE, (b) CEF-GR/CHIT/GCE, and (c) OMCs-CEF/CHIT/GCE versus time.*

Thus, based on the pH study results shown in Figure 8, a pH of 6.2 was selected as the optimum value. Considering the reported pK_a values for CEF, it can be found that the drug possesses one positive center at pH < 3.0. Accordingly, at such low pH values and upon the negative potential applied, a strong electrostatic

interaction exists between the CEF molecule and the electrode surface. However, the calculations show that over a pH range of 3.2 >pH>3.0, the CEF molecule possesses one positive and one negative center, in pH range of 4.1>pH>3.2 it has one positive and two negative centers and, finally, at pH>4.1 the molecule has three negative and one positive centers. Thus, the electrostatic repulsion between the electrode surface and CEF is increased with increasing pH of the solution, which makes the situation suitable for drug release at negative potentials applied to the surface of the electrode in neutral solutions of pH 6.2.

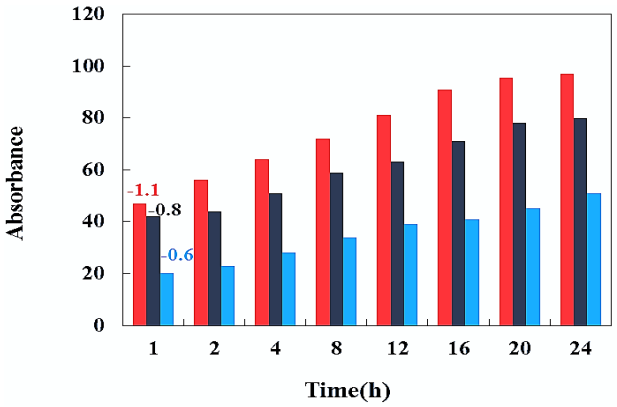

Figure 6. *Cumulative drug release from CEF-OMCs/CHIT/GCE verses time at various applied negative potentials: (a) -1.1 V, (b) -0.8 V, (c) -0.6 V.*

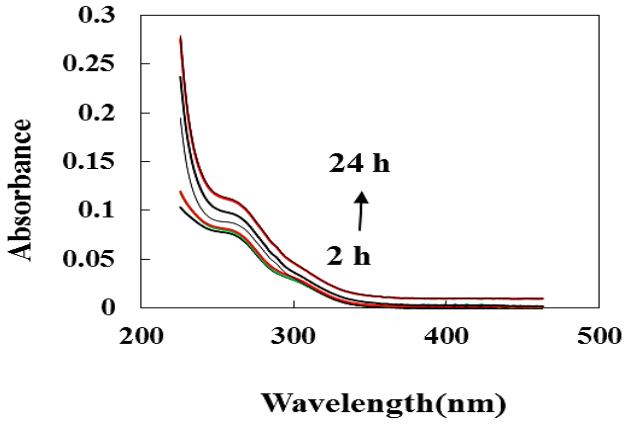

Figure 7. *UV spectra of drug released by electrical stimulation at −1.1 V after 2, 4, 6, 8, 12, and 24 h release in phosphate buffer solution of pH 6.2.*

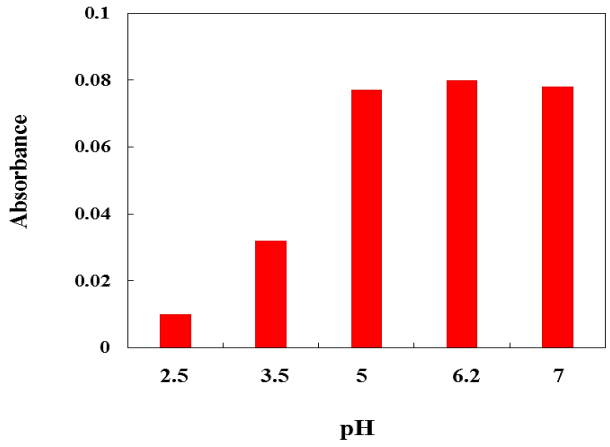

Figure 8. *Effect of pH on drug release of CEF-OMCs/CHIT/GCE at the applied potential of -1.1 V.*

Conclusion

The GR and, especially, OMCs have been receiving much attention in both scientific researches and practical applications owing to their extremely high surface area, which makes them a suitable candidate for applications in controlled drug release. In this work, the controlled release of CEF from the surface of the OMCs-CEF/CHIT/GCE, GR-CEF/CHIT/GCE, and CHIT/GCE electrodes, which can load the drug at the different surface to volume matrices was adopted. The CEF drug was loaded into chitosan hydrogels in the absence and presence of OMCs and GR at GCEs, and then the release of the drug into phosphate buffer solution of pH 6.2 was studied. The OMCs and GR found to act as a diffusion barrier to CEF and slowing down its release when no electrical potential was applied (passive release). Furthermore, the release of CEF could be accelerated compared with the passive diffusion rate by negatively charging the supporting composite and inducing electrostatic repulsion.

Acknowledgment

The authors gratefully acknowledge the Research Council of Kermanshah University of Medical Sciences for financial support. Also, the authors appreciate the Clinical Research Development Center experts at Imam Khomeini and Dr. Mohammad Kermanshahi Hospitals for their cooperation in the preparation of samples.

References

1. S. P. Sherlock, S. M. Tabakman, L. Xie, and H. Dai, *Acs Nano.*, 5, **2011**, 1505-1512.
2. M. S. Yavuz, Y. Cheng, J. Chen, C. M. Cobley, Q. Zhang, M. Rycenga, J. Xie, C. Kim, A. G. Schwartz, and L. V. Wang, *Nature Mater.*, 8, **2009**, 935.
3. T. Hoare, J. Santamaria, G. F. Goya, S. Irusta, D. Lin, S. Lau, R. Padera, R. Langer, and D. S. Kohane, *Nano Lett.*, 9, **2009**, 3651.
4. C. R. Thomas, D. P. Ferris, J. -H. Lee, E. Choi, M. H. Cho, E. S. Kim, J. F. Stoddart, J. -S. Shin, J. Cheon, and J. I. Zink, *JACS*, 132, **2010**, 10623.
5. B. C. Thompson, S. E. Moulton, J. Ding, R. Richardson, A. Cameron, S. O'leary, G. G. Wallace, and G. M. Clark, *J. Control. Releas.*, 116, **2006**, 285.
6. S. Naficy, J. M. Razal, G. M. Spinks, and G. G. Wallace, *Sensor. and Actuat. A-Phys.*, 155, **2009**, 120.
7. D. Esrafilzadeh, J. M. Razal, S. E. Moulton, E. M. Stewart, and G. G. Wallace, *J. Control. Releas.*, 169, **2013**, 313.
8. X. Luo and X. T. Cui, *Electrochem. Commun.*, 11, **2009**, 1956.
9. Y. Kong, H. Ge, J. Xiong, S. Zuo, Y. Wei, C. Yao, and L. Deng, *Appl. Clay Sci.*, 99, **2014**, 119.
10. H. -W. Liu, S. -H. Hu, Y. -W. Chen, and S. -Y. Chen, *J. Mater. Chem.*, 22, **2012**, 17311.
11. C. L. Weaver, J. M. LaRosa, X. Luo, and X. T. Cui, *ACS Nano*, 8, **2014**, 1834.
12. Z. -J. Fan, W. Kai, J. Yan, T. Wei, L. -J. Zhi, J. Feng, Y. -m. Ren, L. -P. Song, and F. Wei, *ACS Nano*, 5, **2010**, 191.
13. X. Huang, S. Wu, and X. Du, Carbon, 101, **2016**, 135.
14. J. Liu, L. Cui, and D. Losic, *Acta Biomater.*, 9, **2013**, 9243.
15. W. Zhu, Q. Zhao, X. Zheng, Z. Zhang, T. Jiang, Y. Li, and S. Wang, *Asian J. Pharm. Sci.*, 9, **2014**, 82.
16. J. You, G. Zhang, and C. Li, *ACS Nano*, 4, **2010**, 1033.
17. R. Langer, *Nature*, 392, **1998**, 5.
18. A. Bianco, K. Kostarelos, and M. Prato, *Curr. Opin. Chem. Biol.*, 9, **2005**, 674.

19. J. S. Im, B. C. Bai, and Y. -S. Lee, *Biomaterials*, 31, **2010**, 1414.
20. S. Jun, S.H. Joo, R. Ryoo, M. Kruk, M. Jaroniec, Z. Liu, T. Ohsuna, and O. Terasaki, *JACS*, 122, **2000**, 10712.
21. W. S. Hummers Jr and R. E. Offeman, *JACS*, 80, **1958**, 1339.
22. D. C. Marcano, D. V. Kosynkin, J. M. Berlin, A. Sinitskii, Z. Sun, A. Slesarev, L. B. Alemany, W. Lu, and J. M. Tour, Improved synthesis of graphene oxide, *ACS Nano*, 8, **2010**, 4806.
23. A. J. Bard, L. R. Faulkner, J. Leddy, and C. G. Zoski, Wiley, (1980), New York.
24. X. Gao, W. Wei, L. Yang, and M. Guo, *Electroanalysis*, 18, **2006**, 485.
25. H. Chai, X. Peng, T. Liu, X. Su, D. Jia and W. Zhou, RSC Adv., **2017**, 7, 36617.